Digest Journal of Nanomaterials and Biostructures Vol. 9, No. 4, October - December 2014, p. 1623 - 1637

INCLUSION COMPLEXES OF HESPERIDIN WITH HYDROXYPROPYL-β - CYCLODEXTRIN. PHYSICO-CHEMICAL CHARACTERIZATION AND BIOLOGICAL ASSESSMENT

A. CORCIOVA[a], C. CIOBANU[a], A. POIATA[a], A. NICOLESCU[b], M. DROBOTA[b], C.D. VARGANICI[b], T. PINTEALA[a], A. FIFERE[b], N. MARANGOCI[b*], C. MIRCEA[a]

[a] *"Grigore T. Popa" University of Medicine and Pharmacy, 16, University Street, 700115 Iasi, Romania*

[b] *"Petru Poni" Institute of Macromolecular Chemistry, 41A, Grigore Ghica-Voda Alley, 700487 Iasi, Romania*

The aim of this research was to prepare the inclusion complexes formed by hesperidin and (2-hydroxypropyl)-β-cyclodextrin by different techniques (kneading, co-evaporation and lyophilization methods), to carry out phase solubility studies, *in vitro* dissolution, antioxidant and antimicrobial tests. To confirm the inclusion compounds formation, spectroscopic (UV-Vis, FTIR, ^{1}H-NMR) and thermal (DSC) methods were used. The obtained thermodynamic parameters proved that the inclusion process is spontaneous and is influenced both by temperature and cyclodextrin concentration. Moreover, for all obtained inclusion complexes the dissolution of hesperidin increased, the process being more effective for the lyophilization method in gastric pH 1.2 medium. Also, the inclusion complexes presented improved antimicrobial and antioxidant activities as compared to free hesperidin. The best antimicrobial activity was obtained against *Candida albicans* for the compound obtained by co-evaporation. The compound obtained through lyophilization showed an enhanced antioxidant activity according to the results obtained through two methods (DPPH free radical scavenging assay and lipoxygenase inhibition assay), while through the third technique (determination of the reducing capacity) the best results were obtained for the compound prepared by kneading. Thus, hydroxypropyl-β-cyclodextrin can be used to improve the biological properties of hesperidin.

(Received October 9, 2014; Accepted December 5, 2014)

Keywords HP-β-cyclodextrin; Hesperidin; Inclusion complex; Antimicrobial activity; Antioxidant activity, *In vitro* dissolution profile

1. Introduction

Flavonoids are a large class of natural polyphenolic compounds characterized by a flavan nucleus, which have low molecular weight and are widely distributed in fruits, vegetables, teas, wines, etc [1, 2]. The bioflavonoid hesperidin (5, 7, 3'- trihydroxy - 4'- methoxy - flavanone 7 – rhamnoglucoside), a flavanone glycoside containing a flavanone (hesperitine) and a disaccharide (rutinose) was first discovered in 1827 by Lebreton [3]. Hesperidin is the main flavonoid found in sweet oranges and lemons and also an inexpensive secondary compound of citrus cultivation [4]. Currently, hesperidin (HES) is used as an auxiliary treatment in many diseases and its deficiency has been associated with pain in the extremities, low capillary resistance, tiredness and night muscle cramps [5]. It has been reported that HES has various pharmacological and biological properties such as anti-inflammatory, cardiovascular [6] and antioxidant effects [7]. It was also

* Corresponding author: nmarangoci@icmpp.ro

found to possess venotonic and vasculo-protective properties [8] as well as beneficial effects in hemorrhoidal disease [9]. Some previous studies have showed that HES reduces cholesterol [10], blood pressure [11] and even decreases bone density loss in rats and mice [12]. Additionally, HES was reported to possess significant analgesic, antifungal, antiviral and neuroprotective properties [13] and also the ability to suppress cell proliferation in oral carcinogenesis [14]. Following oral administration, HES is absorbed through the gastrointestinal tract, however, low bioavailability was recorded (< 25 %). This is probably due to the fact that it has poor water solubility and it precipitates in acidic environment [15]. Therefore, it is important to develop new methods for enhancing the solubility of HES.

Cyclodextrins are cyclic oligosaccharides obtained biotechnologically from the enzymatic degradation of starch using a glucosyltransferase most commonly derived from *Bacillus macerans* [16]. They consist of six (α-cyclodextrins), seven (β-cyclodextrins) and eight (γ-cyclodextrins) glucopyranose monomers which are linked by α-(1, 4) bonds. Cyclodextrins have a hydrophilic outer surface and a hydrophobic cone-like central cavity and are well known for their abilities to form inclusion complexes with various organic/inorganic molecules [17]. While the outer surface is polar due to the presence of the primary and secondary hydroxyls located on the ring's edge, the inner surface is non-polar due to the presence of glycosidic oxygens and methine protons. This increases drug solubility in aqueous solutions, chemical stability and bioavailability. Because of these improvements, the cyclodextrines have received special attention in numerous pharmaceutical applications [18]. Hydroxypropyl-β-cyclodextrin (HP-βCD), a hydroxyalkyl derivate, is used as an alteranative to β-cyclodextrin and is obtained through the reaction of propylene oxide and β-cyclodextrin in alkaline aqueous solutions. Compared with other cyclodextrins (α, β, γ), HP-βCD is known to have improved water solubility properties (> 60 %) [19]. Moreover, recent studies have shown that HP-βCD are toxicologically safe both in humans and animals when administered either orally or intravenously [19, 20].

Continuing the research in the field of the inclusion complexes obtained by combining flavonoids and cyclodextrins, the main purpose of this research was to report the preparation and characterization of the inclusion complexes formed by HES and HP-βCD. The HES - HP-βCD inclusion complexes were prepared by three different methods (kneading, co-evaporation and lyophilization) and confirmed by Fourier transform infrared spectroscopy (FTIR), nuclear magnetic resonance spectroscopy (^{1}H-NMR) and differential scanning calorimetry (DSC). In order to investigate whether the biological properties of HES were influenced by the presence of HP-βCD, we have performed several tests, such as: antimicrobial, antioxidant and *in vitro* dissolution tests for the obtained inclusion compounds *versus* free HES. For this purpose we used similar physiological conditions (a pH 1.2 medium in order to simulate the gastric fluid and a pH 6.8 medium for the intestinal fluid). Moreover, the results obtained by complexation with HP-βCD were compared to our previous published results on the complexation of hesperidin with βCD [21].

2. Experimental

Materials: Hesperidin (HES) and hydroxylpropyl-β-cyclodextrin (HP-βCD) were obtained from Sigma Aldrich Company (USA) and were used as received without any prior purification. HES, with a purity ≥ 80 %, had the following characteristics: ((2*S*)-5-hydroxy-2-(3-hydroxy-4-methoxyphenyl)-7-[(2*S*,3*R*,4*S*,5*S*,6*R*)-3,4,5-trihydroxy-6-[[(2*R*,3*R*,4*R*,5*R*,6*S*)-3,4,5-trihydroxy-6-methyloxan-2-yl]oxymethyl]oxan-2-yl]oxy-2,3-dihydrochromen-4-one). All other solvents and reagents were of analytical grade.

Preparation of HP-βCD inclusion complexes

For the preparation of the inclusion complexes, three methods were employed: co-evaporation, kneading and lyophilization, using a 1:1 molar ratio. The conditions were the same as for the preparation of HES-βCD inclusion complexes, which were previously published [21].

Kneading (KN) method: HES and HP-βCD powders were wetted with an appropriate volume of water, mixed until a paste was obtained and after that it was stirred until the water evaporated.

Co-evaporation (CV) method: the accurately weighed HP-βCD was dissolved in distilled water and a saturated solution was obtained. After that, the ethanolic solution of HES was added slowly and under stirring over the HP-βCD solution. The mixture was stirred at 30 ^{0}C for 24 hours, after which the temperature was decreased to 25 ^{0}C and stirred until the solvent evaporated. The obtained mass was dried at 40 ^{0}C in an oven until constant weight. The dried complex was grounded to a fine powder.

Lyophilization method: HES and HP-βCD were mixed in an aqueous solution and magnetically stirred for 72 hours to allow the complex formation. After mixing, the solution was frozen at – 40 ^{0}C and lyophilized in a VirTis Freeze Mobile 6.6 (Virtis Co., USA) until all the moisture had been sublimated.

Methods

Phase solubility studies: The phase solubility studies were performed according to the method reported by Higuchi and Connors [22], with some modifications. An excess amount of HES was mixed in a series of water solutions of HP-βCD ranging in concentration from 0.684 to 13.69 mM. The vials containing the mixtures were stirred for 24 hours at four temperatures: 20, 25, 30 and 37 ± 1 ^{0}C. In order to determine the concentration of HES, all samples were filtered using a 0.45 μm nylon disc filter, after which the samples were analyzed by UV-Vis spectrophotometry at 286 nm using proper calibration curves. The phase solubility diagrams were obtained by plotting the concentration of HES *vs* the concentration of HP-βCD at 20, 25, 30 and 37 ± 1 ^{0}C. The experiments were carried out in triplicate for each temperature.

Physico-chemical inclusion compounds characterization

- The UV-Vis absorption spectra were recorded using a double beam Jasco UV-Vis 530 spectrophotometer with 1.0 cm quartz cells and scan speed of 1000 nm min^{-1}. The solutions were scanned in the range of 200-400 nm

- Fourier Transform Infrared Spectroscopy spectra were collected between 4000 to 500 cm^{-1} (Mid infrared region) on a Bruker Vertex 70 device, equipped with ATR device (Golden Gate, Bruker) via Attenuated Total Reflectance (ATR) technique. Smoothing of the spectra and baseline correction were applied.

- ^{1}H-NMR measurements were performed using a DRX 400 Avance Bruker 400 MHz spectrometer.

- DSC measurements were carried out in a stream of nitrogen atmosphere on a DSC 200 F3 Maia differential scanning calorimeter (Netzsch, Germany). The accurately weighed sample (10 mg) was heated in pressed and pierced aluminum crucibles, at a scanning rate of 10 ^{0}C min^{-1} and a nitrogen flow rate of 50 mL min^{-1}. The device was calibrated for temperature and sensitivity with indium, according to standard procedures.

Calculation of thermodynamic parameters of the inclusion of HES into HP-βCD cavity

The thermodynamic parameters of the reaction: Gibbs free energy change (ΔG^0_{tr}), free energy change (ΔG^0), enthalpy change (ΔH^0) and entropy change (ΔS^0) were calculated using the stability constant's temperature dependence using equations 1-5 [23-26]:

$$\Delta G^0_{tr} = - RT \log \frac{S}{S_0} \quad (1)$$

where: ΔG^0_{tr} - Gibbs free energy change (kJmol^{-1}); R - the gas constant (Jmol^{-1}K^{-1}); T - the absolute temperature of the reaction (K); S/S_0 = was the ratio between the solubility of HES in HP-βCD water solution and the solubility of HES in water.

$$\Delta G^0 = -2.303\,RT \log K_s \quad (2)$$

where: ΔG^0 - Gibbs free energy ($kJmol^{-1}$); R = the gas constant ($Jmol^{-1}K^1$); T - the absolute temperature of the reaction (K); K_s - the equilibrium constant of the complex formed with 1:1 stoichiometry (M^{-1}).

$$Slope = \frac{\Delta H^0}{2.303R} \quad (3)$$

where: Slope - slope of log Ks versus 1/T line graph; ΔH^0 - enthalpy change ($kJmol^{-1}$); R - the gas constant ($Jmol^{-1}K^{-1}$)

$$\log Ks = -\frac{\Delta H^0}{RT} + \frac{\Delta S^0}{R} \quad (4)$$

where: K_s - the equilibrium constant of the complex formed with 1:1 stoichiometry (M^{-1}); ΔH^0 - enthalpy change ($kJmol^{-1}$); R - the gas constant ($Jmol^{-1}K^{-1}$); ΔS^0 - entropy change ($Jmol^{-1}K^{-1}$); T - the absolute temperature of the reaction (K).

$$\Delta G^0 = \Delta H^0 - T\Delta S^0 \quad (5)$$

where: ΔG^0 - Gibbs free energy ($kJmol^{-1}$); ΔH^0 - enthalpy change ($kJmol^{-1}$); T - the absolute temperature of the reaction (K); ΔS^0 - entropy change ($Jmol^{-1}K^{-1}$).

Biological characterization of the inclusion compounds

The antimicrobial activity was performed by the agar diffusion method using *Staphylococcus aureus (S. aureus)* ATCC (American Type Culture Collection) 25923, *Escherichia coli (E. coli)* ATCC 25922 and *Candida albicans (C. albicans)* ATCC 10231 as test microorganisms. Mueller-Hinton agar was used as medium for bacteria and Sabourand maltose agar for fungi. Each microorganism was tested in triplicate.

The antioxidant activity of the prepared inclusion compounds was evaluated using three methods:

- method 1 - DPPH (2, 2 diphenyl-picryl-hydrazyl) radical scavenging activity [27] – the scavenger activity was calculated using DPPH absorbance and the absorption of the sample treated with DPPH after 10 minutes. For the samples that achieved 50 % scavenger capacity the IC_{50} value was calculated.

- method 2 - determination of the reducing capacity [28] - the IC_{50} value was determined only for the samples that had the absorbance greater than 0.5. The reducing capacity was calculated based on a formula that uses the absorbance and the concentration of the solutions that showed the absorbance just under 0.5 and over 0.5.

- method 3 - lipoxygenase inhibition assay (modified Malterud method) [29] - the ability to inhibit the lipoxygenase activity was calculated using the difference between the absorbance of the enzyme without inhibitor at second 90 and the absorbance of the same solution at second 30 and the difference between the absorbance of the enzyme with inhibitor at second 90 and the absorbance of the same solution at second 30. For each sample the IC_{50} value was calculated, expressed in mM HES in final solution.

The dissolution studies for HES and its prepared inclusion compounds were performed in two types of medium: (a) simulated gastric fluid (0.1 N hydrochloric acid solution, pH 1.2) and (b) simulated intestinal fluid (phosphate buffer, pH 6.8). The HES concentration was determined by UV measurements at 286 nm against a blank containing the used medium. Suitable constructed standard curves were used. All dissolution studies were performed in triplicate. The dissolution diagrams were constructed by plotting mean values of cumulative dissolution of HES *vs* time.

3. Results and discussion

Solubility studies

Through the solubility studies (Fig. 1) conducted at different temperatures (20, 25, 30 and 37 ^{0}C) [23], the effect of HP-βCD on the solubility of HES was investigated, and as a consequence, their solubility diagram type was established. Also, this type of study allowed the calculation of the stability constant for the formed inclusion complex. Figure 1a shows the UV spectrum of free HES and in the presence of increasing amounts of HP-βCD. A bathochromic displacement of the characteristic peak of HES from 284 nm to 286 nm (called band II in flavonoids), and the appearance of a shoulder around 330 nm (called the band I in flavonoids) were observed. The measurements were carried out taking into consideration the band II of HES, due to its origins in the benzoyl ring's electronic transitions [30]. The maximum absorbance shift can be attributed to the HES transfer or to a part of its molecule from the solution to the HP-βCD cavity, with the formation of weak interactions (hydrogen type bonds, van deer Waals forces, hydrophobic interactions, etc). The same maximum absorption shift was observed in the case of the inclusion of HES into βCD cavity [21].

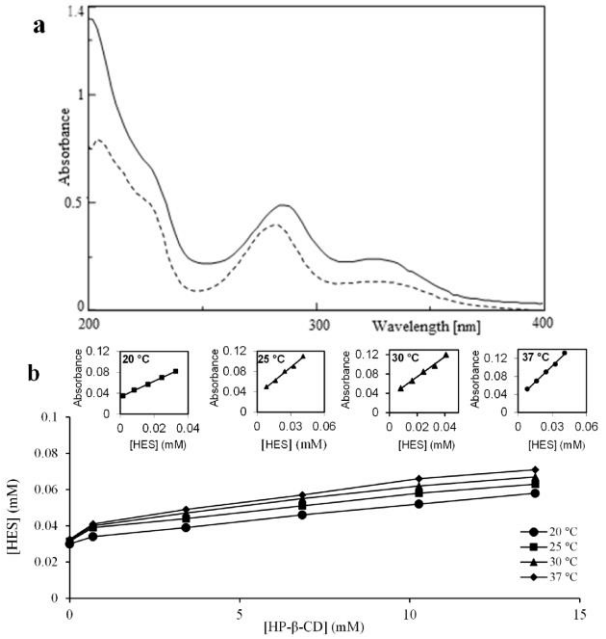

Fig. 1. UV-Vis spectra of free HES and in the presence of HP-βCD (a); Phase solubility diagrams for water solutions of HES versus HP-βCD concentration at different temperatures (20, 25, 30 and 37 ± 1 ^{0}C) (b). Inset: Calibration curves of HES in water at different temperatures (20, 25, 30 and 37 ± 1 ^{0}C).

From the solubility diagrams (Figure 1b) it can be seen that the solubility of HES in water increases linearly with the increment of cyclodextrin concentration and temperature. This demonstrates the formation of A_L type solubility curves which is in agreement with Higuchi and Connors's theory [22]. Given the fact that in all 4 cases the slopes of the curves were less than 1, the solubility increase may be attributed to the formation of a 1:1 inclusion complex between HES and HP-βCD in aqueous solution. The stability constants (Ks) were calculated using equation 6, from the linear portion of the solubility diagrams (22):

$$Ks = \frac{slope}{S_0\,(1-slope)} \tag{6}$$

where: slope – was calculated from the graph; S_0 – HES intrinsic solubility in the absence of HP-βCD.

The following Ks values were obtained: 169.66 M^{-1} at 20 ^{0}C, 198.12 M^{-1} at 25 ^{0}C, 217.66 M^{-1} at 30 ^{0}C and 242.49 M^{-1} at 37 ^{0}C, showing that in all cases there were favorable conditions for the formation of inclusion complexes. The stability constant value at 25 ^{0}C is between the one obtained by Tommasini et al. [31] (60 M^{-1}) and the one obtained by Majumdar et al. [32] (625 M^{-1}); these differences could be attributed to different working conditions (different periods and types of agitation).

On comparing the Ks values for the inclusion complexes obtained between HES and βCD [21] to those obtained between HES and HP-βCD, for the same temperature, a higher stability of the inclusion complexes of HES with HP-βCD was observed, indicating a better stability of the complex when HP-βCD was used. Moreover, calculating the thermodynamic parameters of the inclusion process (Table 1), using equations 1-5, the interaction forces between HES and HP-βCD can be confirmed. As in the case of the hesperidin inclusion into βCD cavity [21], the negative values of ΔG^0_{tr} and ΔG^0 were obtained, demonstrating that the formation of the HES with HP-βCD inclusion complex is a process that occurs spontaneously at a chosen temperature and the working conditions were favorable for the HES's solubilization. Also, the positive values of ΔH^0 and ΔS^0 parameters indicate that the inclusion process is controlled by enthalpy and it takes place through the establishment of hydrophobic interactions between HES and HP-βCD molecules, when the HES is transferred from aqueous medium to the hydrophobic cyclodextrin cavity [23-26].

Table 1. Thermodynamic parameters of the inclusion complexes formation between HES and HP-βCD

Temperature ^{0}C (K)	[HP-βCD] (mM)	20 ^{0}C (293 K)	25 ^{0}C (298 K)	30 ^{0}C (303 K)	37 ^{0}C (310 K)
ΔG^0_{tr} (kJmol^{-1})	0.684	- 0.131	- 0.222	- 0.244	- 0.257
	3.42	- 0.277	- 0.354	- 0.413	- 0.461
	6.84	- 0.449	- 0.517	- 0.587	- 0.626
	10.27	- 0.542	- 0.654	- 0.723	- 0.734
	13.69	- 0.717	- 0.745	- 0.806	- 0.871
ΔG^0 (kJmol^{-1})		- 12.504	- 13.106	- 13.558	- 14.150
ΔS^0 (Jmol^{-1})		45.97	47.22	47.93	48.76
ΔH^0 (kJmol^{-1})	0.9669				

Physico-chemical inclusion compounds characterization

Fourier transform infrared spectroscopy (FTIR)

The FTIR analysis is a useful method to confirm the formation of the inclusion complexes [33, 34]. As a general observation, the modifications in the FTIR spectra of the inclusion complexes compared with those of the individual compounds could give information on the complex formation [35]. The FTIR spectra of HES, HP-βCD and their inclusion complexes obtained by different techniques are presented in Figure 2A.

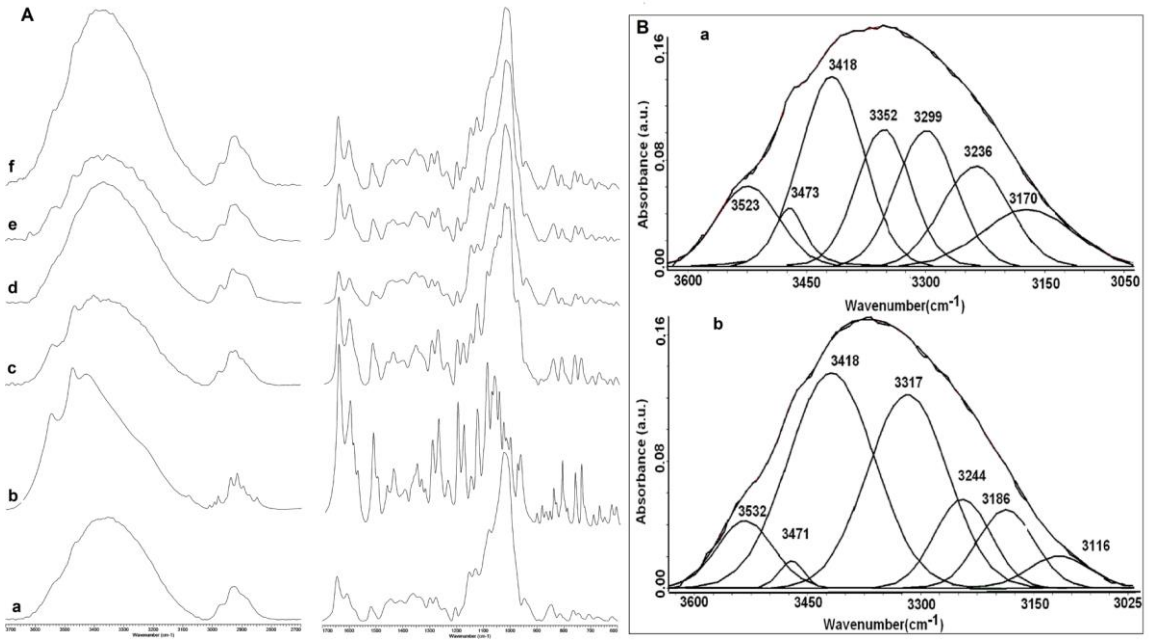

Fig. 2. A. Comparative FTIR spectra of HP-βCD (a); HES (b); physical mixture (c); L (d), KN (e); CV (f). B. Deconvoluted FTIR spectra in 3600-3000 cm^{-1} interval for HP-βCD (a) and L (b).

The undeconvoluted and deconvoluted FTIR spectra of the HP-βCD (Figure 2 and 3) showed prominent absorption bands at 3418, 3352 and 3170 cm^{-1} of O-H stretching vibrations, 2930 cm^{-1} of C-H stretching vibrations, at 1374, 1359, 1339, 1324, 1299, 1277, 1257 and 1240 cm^{-1} due to the different vibrations of C-H groups and at 1154, 1085, 1036 cm^{-1} for C-O stretching vibrations. The bands at 1464, 1277 and 850 cm^{-1} are a consequence of the hydrogen bonds formation between primary and secondary OH groups of HP-βCD located at 3418, 3352 and 3170 cm^{-1} and these hydrogen bonds produced new vibration bands at 3523 and 3299 cm^{-1}. The other bands from 3600-3050 cm^{-1} interval are specific for the water molecules which are located inside the cavity of cyclodextrin. In the FTIR spectrum of HES, characteristic absorption bands were present at 3403 and 3534 cm^{-1} (OH stretching vibrations), 2919 cm^{-1} (CH and CH_2 aliphatic), 1645 and 1607 cm^{-1} (C=O in cetone) and at 1605, 1594, 1576 cm^{-1} (C=C valence vibrations in the benzene rings). The absorption bands in 950-700 cm^{-1} interval are specific for the pulsation vibrations in glucopyranosyl unit and for the deformation vibrations of C-H bonds [36]. In the FTIR spectra of the inclusion complexes, the specific bands of HP-βCD and HES are modified and reduced in their intensities due to the decreasing of the number of water molecules involved in the hydrogen bonding formation and maybe due to the formation of hydrogen bonds between HES and cyclodextrin, suggesting that the water molecules from the cavity of cyclodextrin were replaced by HES. This observation is sustained by the relevant changes in the deconvoluted FTIR spectra of L inclusion complex in 3600-3000 cm^{-1} interval (Figure 2B).

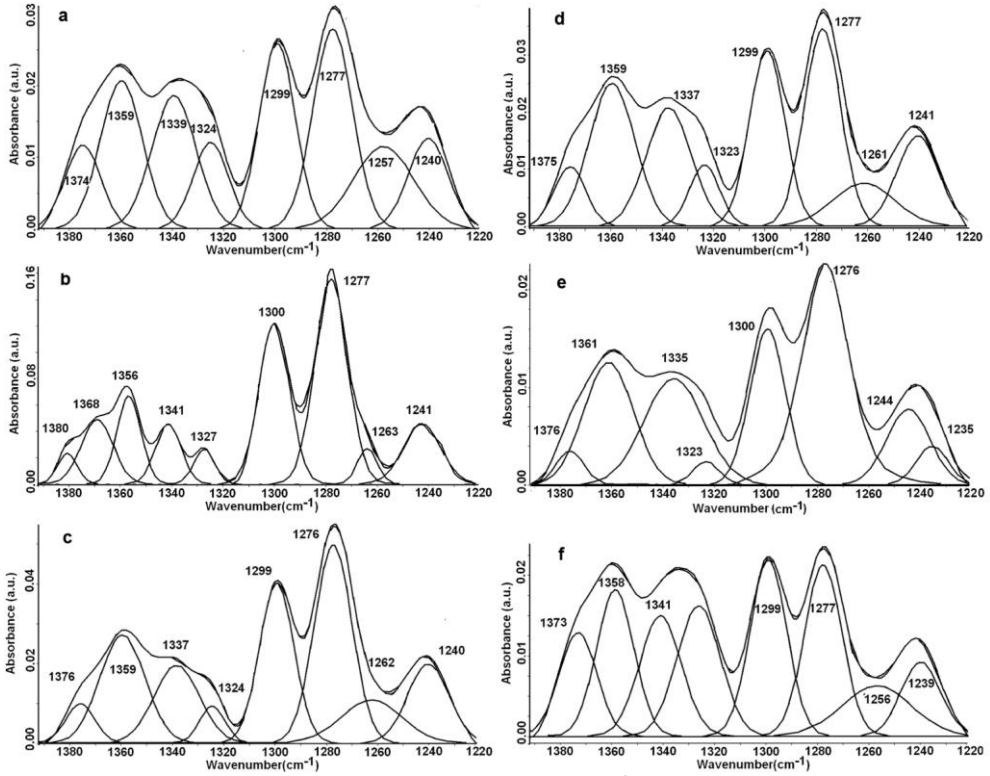

Fig. 3. Deconvoluted FTIR spectra in 1400 - 1200 cm^{-1} interval for HP-βCD (a); HES (b); physical mixture (c); KN (d); CV (e); L (f).

Comparing the deconvoluted spectrum of HES with those of HP-βCD in the 1400-1200 cm^{-1} interval (Figure 3), HES presented a sub-band at 1380 cm^{-1}, most likely derived from the absorption bands induced by the deformation vibrations of C-H group linked to the primary hydroxyl group of HES. For the inclusion complexes (Figure 3), one can observe eight sub-bands that reflect the contribution of HP-βCD and HES compounds in their structures. In the case of the deconvoluted FTIR spectra of HES-HP-βCD inclusion complexes, the OH vibrations caused by the activation lead to different interactions and also to a connectivity of the involved bonds, which was materialized into a transition to a higher frequency, which demonstrates a less structured compound. The presence of the stretching vibrations of C-O-C in 1250-1300 cm^{-1} interval is indicated by a relative extended and decreased intensity in the inclusion complexes (due to the asymmetric stretching vibrations of C–O–C group). It should be noted that, also, the band from 1277 cm^{-1} which is attributed to C=O group from HES is present in a decreased intensity, as compared with those of HES showing that the C=O group is present in a different environment. The bands from 1200-1250 cm^{-1} interval are assigned to the stretching and deformation vibrations of the ether units. The changes in the vibrational frequencies could be attributed to the decreasing of the inter-atomic bonds as a consequence of an altered environment that induces the formation of new intermolecular hydrogen bonds (as an example between HES and HP-βCD). Also, monitoring the characteristic bands for the vibrations located at around 1340 cm^{-1} and around 1370 cm^{-1} from the FTIR deconvoluted spectra (Figure 3), we can observe the appearance of some changes that seems to indicate the formation of a new supramolecular structure.

Nuclear magnetic resonance spectroscopy (^{1}H-RMN)

One of the most used method to reveal the interaction between cyclodextrins (as a host) and HES (as a guest) is ^{1}H-NMR spectroscopy, showing the protons' displacement signals of both host and guest molecules [34, 37, 38].

The comparative ^{1}H-NMR spectra of HP-βCD, HES and HES-HP-βCD are shown in Fig. 4. Table 2 presents the movements of the proton signals from the methoxy group and the

protons of the aromatic ring substituted with the methoxy group from HES, in the absence and the presence of HP-βCD, using a HES:HP-βCD molar ratio of 1:1 and 1:3.

Table 2. The chemical shifts of the interest signals for HES in the absence and presence of HP-βCD.

δ (ppm)	HES	Molar ratio HES-HPβCD	
		1:1	1:3
OCH3	3.7821	3.7819	3.7812
Substituted aromatic ring with OCH3	6.8969-6.9629	6.8965-6.9626	6.8959-6.9621

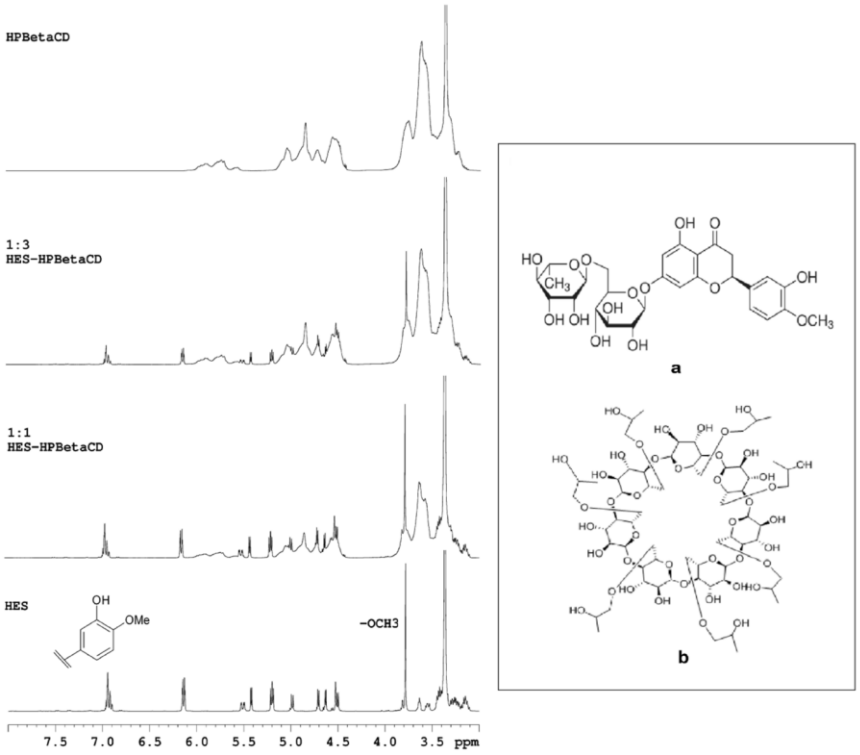

Fig. 4. ^{1}H-NMR spectra of HP-βCD, HES and their mixture at different molar ratio; Inset: HES (a) and HP-βCD (b) structures.

Small values of protons' movements can be observed, more pronounced in the case of a 1:3 molar ratio, while the other peaks remained almost unchanged. It can be said that, after the combination of HES with HP-βCD, an inclusion process of the aromatic ring substituted with methoxy of HES into cyclodextrin cavity was observed.

Differential scanning calorimetry (DSC)

The DSC method reveals some information on host–guest solid state interactions. By comparing the DSC curves (Figure 5), the differences between free substances and inclusion compounds may be identified (differences that occur *via* phase transformations during heating). The occurring of the complexation is usually evidenced by the decreased intensities or disappearance of the drug melting temperature. As it can be observed from Figure 5, for HES, a dehydration peak is exhibited at 121 ^{0}C and a melting peak at 262 ^{0}C while HP–βCD shows a broad endothermic peak at 97 ^{0}C, corresponding to the water elimination from the cyclodextrin cavity. In the inclusion complexes, the dehydration peak of HP–βCD is shifted to lower temperature domains, being the first indication that a host-guest interaction occurred. In the case of HES-HP–βCD inclusion complexes, the HES dehydration peak also appears in the rest of the

compounds, with reduced intensity, exhibiting significant shifts compared to that of pure HES dehydration (121 ^{0}C). The two glycosidic moieties in the HES structure may couple with the hydrophilic exterior and/or the hydroxypropyl moiety of the HP–βCD, *via* OH groups, with hydrogen bond formation and the rest of the HES molecule entering in the HP–βCD cavity. HP–βCD exhibited an endothermic transition centered at 224 ^{0}C, attributed to a glass transition (T_g), aspect which is consistent with the reported literature [39-41]. It is a known fact that the T_g of an amorphous compound is usually sensitive to the presence of the foreign molecules if significant physical host–guest molecules interactions can be observed. In this sense, one may observe that in the inclusion compounds the T_g of HP–βCD shifts significantly to different temperature domains and broadens its intensity, aspect confirmed by an increase in heat capacity (ΔC_p, J g^{-1} $^0C^{-1}$) values in the following order: HP–βCD (0.402) < KN (0.656) < L (0.806) < CV (0.935). The displacement and broadening of the T_g corresponds to an increase in amorphous phase upon complexation. Furthermore, the melting peak of pure HES disappears and a new endothermic peak appears in the inclusion compound, slightly overlapping with the T_g, indicating possible inclusion complex formation or an interaction between HES and HP–βCD molecule in solid state due to the formation of a new amorphous phase [42].

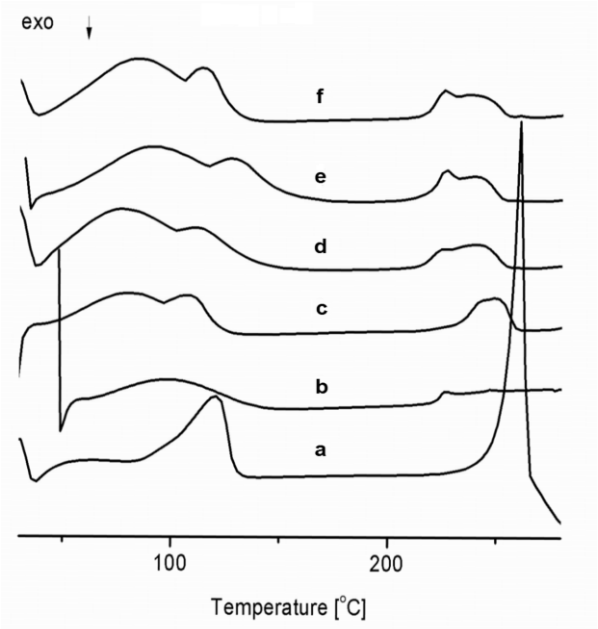

Fig. 5. DSC curves of: HES (a); HP–βCD (b); physical mixture (c); KN (d); CV (e); L (f).

Biological characterization of the inclusion compounds

Antimicrobial activity

The inclusion complexes' antimicrobial activity compared to free HES against *S. aureus*, *E coli* [43] and *C.albicans* [44] is presented in Figure 6. All tested microorganisms were susceptible to HES and its inclusion complexes. As in the case of the inclusion complexes obtained with βCD, an increased antimicrobial activity was observed for the inclusion compounds with HP-βCD, but lower than the ones with βCD [21]. In both cases, the antimicrobial activity of HES and its complexes obtained with βCD or HP-βCD was in the following order: *C. albicans* > *S. aureus* > *E. coli*. The bacterial wall composition influences in a very important way the antimicrobial activity of HES and its inclusion complexes. The cell wall of *E. coli* consists of an outer layer of phospholipids, liposaccharides and lipoproteins while the inner layer consists of a thin layer of peptidoglycan which makes it harder to be permeated by HES. The cell wall of *C. albicans* contains perpendicularly aligned polysaccharidic fibrils with a hydrophobic surface and

two classes of proteins that are covalently attached to that network of structural fibrillar polysaccharides. This structure probably makes it easy to be penetrated by HES [45].

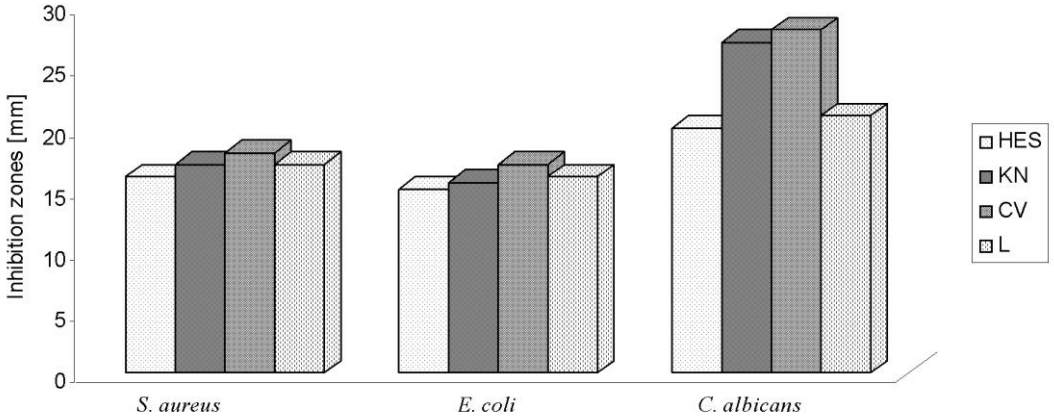

Fig. 6. Antimicrobial activity (inhibition zones – mm) for HES and its inclusion complexes on the tested microorganisms

Moreover, the method of preparation affects the complexes' solubility therefore influencing HES's availability to the tissue. The best activity was recorded in the case of the complexes with HP-βCD obtained by co-evaporation.

Antioxidant activity

For the DPPH free radical scavenging assay (method 1) and for the reducing capacity (method 2) we used seven different concentrations, in range of 0.5118 – 32.756 mM. The lipoxygenase inhibition (method 3) assay was performed using a spectrophotometric method at five different concentrations which varied between 0.5118-8.189 mM. HES and HP-βCD were used as controls. The results are shown in Figure 7. The calculated values of IC_{50} for the used methods depending on the inclusion method are presented in Table 3.

Method 1: One of the most widely used methods to determine the antioxidant activity is based on the reaction of 2, 2 diphenyl-picryl-hydrazyl. The method is based on the reduction of DPPH radical by HES and HP-βCD which contain hydroxyl groups. An increase in HES's scavenger capacity with increasing its concentration and an improvement in the antioxidant properties of the inclusion complexes can be observed (Figure 7a). When HES is conjugated with HP-βCD, hydrogen bonds can be formed These hydrogen bonds weaken the covalent bonds between hydrogen and oxygen from the OH groups, which in turn would make the donation of hydrogen from the HES's OH groups more easy [46-48].

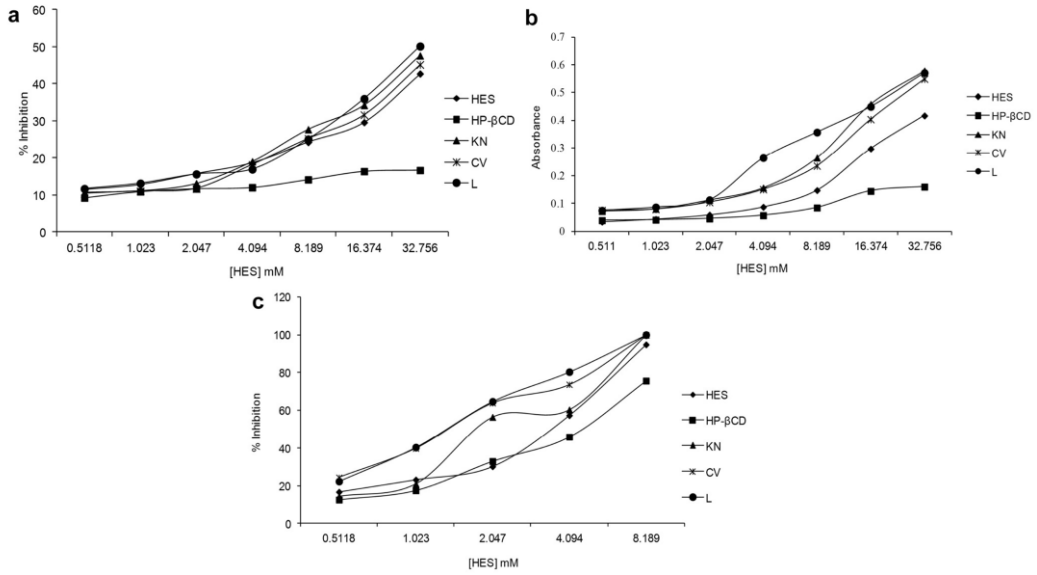

Fig. 7. Determination of DPPH radical scavenging activity (a); reducing ability (b) and inhibition of lipoxygenase activity (c) for the tested compounds, compared with free HES and HP-βCD.

Table 3 IC_{50} values for the analyzed compounds.

Method/Sample	KN	CV	L	HP-βCD	HES
Method 1 (mM)	-	-	3.251 ± 012	-	-
Method 2 (mM)	2.501 ± 0.021	3.088 ± 0.011	2.627 ± 0.015	-	-
Method 3 (mM)	0.0301 ± 0.55	0.0229 ± 0.46	0.0224 ± 0.02	0.0314 ± 0.33	0.0565 ± 0.80

As well as in the case of the complex obtained with βCD, the IC_{50} calculation could be realized only for the complex obtained by lyophilization, because for the other compounds the inhibition was smaller than 50 % due to the small concentrations taken into work.

Method 2: In the case of iron reducing capacity measurement [48, 49], the HES from the inclusion complexes showed a more powerful antioxidant activity compared to free HES, especially for the complex obtained by kneading (Figure 7b). This increase in the reducing capacity could be explained by the increment of HES's solubility after its inclusion into cyclodextrin cavity. Just like in the case of the complex obtained with βCD [21], the IC_{50} of the inclusion complexes were calculated while for HES, an absorbance smaller than 0.5 was obtained and therefore could not be calculated its IC50.

Method 3: Another method used to analyze the antioxidant properties of HES is the one in which the activity of lipoxygenase is blocked. This enzyme has an important role in the biosynthesis of leukotrienes which are involved in numerous inflammatory and allergic diseases. The products resulting from the lipoxygenase activities like hydroperoxyeicosatetraenoic acid, hydroxyeicosatetraenoic acid, leukotrienes and lipoxins are involved in the development of diseases such as rheumatoid arthritis, psoriasis, asthmatic reactions and glomerular nephritis [50]. It can be seen that the HES included into the HP-βCD cavity shows a more pronounced capacity to inhibit the lipoxygenase compared to free HES (Figure 7c). This can be explained by the fact that the OH groups of HES and HP-βCD block the iron ions and thus the oxydation of Fe^{2+} to Fe^{3+} doesn't occur, knowing that the action of the enzyme depends on the oxidation state of iron which is involved in the redox reaction [51].

From the calculated IC_{50} values it can be observed that for the inclusion compounds, HES concentrations ranging from 0.0224-0.0301 mM are needed, compared to 0.0565 mM of free HES in order to achieve 50 % inhibition ability. Comparing with the values obtained for βCD, which were in the range of 0.0422-0.0495 mM, one can say that in the case of the inclusion compounds obtained with HP-βCD, the antioxidant activity is increased by at least 2 times.

In vitro dissolution studies

The dissolution profiles of free HES and its inclusion compounds prepared by different methods are presented in a specific period of time (120 minutes) and under physiological conditions, such as simulated gastric fluid pH 1.2 (Figure 8a) and simulated intestinal fluid pH 6.8 (Figure 8b) [52, 53].

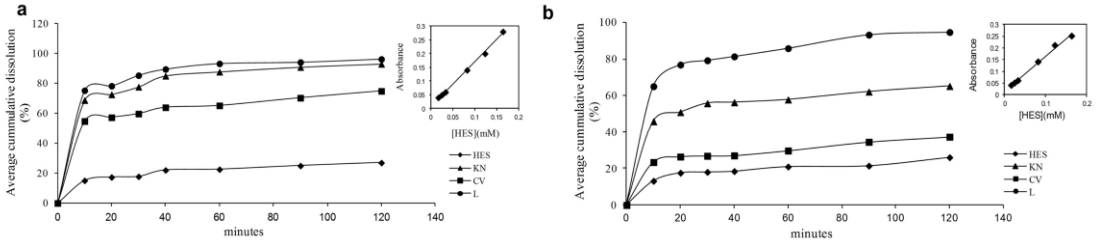

Fig. 8. In vitro dissolution profiles of HES and its inclusion complexes with HP-βCD vs time in 0.1 N HCl (pH = 1.2) (a) and in phosphate buffer at pH = 6.8 (b). Inset a: HES etalon curves in 0.1 N HCl. Inset b: HES etalon curves in phosphate buffer at pH = 6.8.

It can be seen that all inclusion complexes had an improved dissolution rate compared to that of free HES and its variation depends on the inclusion complexes' method of preparation. As well as in the case of the inclusion complexes obtained with βCD, the best rate of dissolution was observed for the lyophilization method in acid medium. HP-βCD exhibits surfactant properties, being hydrophilic on the external surface, resulting in a decrease of the interfacial tension between HES and the dissolution medium, thus resulting in an improvement in the dissolution rate. The dissolution rate was higher for the compounds obtained with HP-βCD, compared to those obtained with βCD. This may be generated by the higher solubility of HP-βCD (generated by the presence of hydroxypropyl radical) than the one of βCD, yielding to more soluble inclusion compounds. Increasing the rate of dissolution in an acid medium can lead to an increased release of HES and to an improved bioavailability of the compound at gastric level.

4. Conclusions

The results of this study demonstrated that HES could be efficiently complexed with HP-βCD. Moreover, the properties of HES were enhanced after its complexation with HP-βCD. According to the phase solubility diagrams, the solubility of HES increased, the best solubility being obtained at 37 ^{0}C. The values of thermodynamic parameters showed that the inclusion of HES into HP-βCD cavity was enhanced when the HP-βCD concentration and the temperature of the process were increased. In addition, *in vitro* studies showed that the inclusion compounds' antibacterial, antioxidant and dissolution properties were enhanced.

In all the studies, a superiority of HP-β-CD compared to β-CD was observed, with the exception of the antimicrobial activity where the inclusion compounds obtained with β-CD proved to be more efficient, but the differences were not significant.

Our results showed that the complexation of HES with HP-βCD through different methods (lyophilization, co-evaporation and kneading) could be a promising technique that can be used to improve the properties of HES and thus, for its future use as an inclusion complex, in pharmaceutical preparations.

Acknowledgments

Scientific research funded by the University of Medicine and Pharmacy "Grigore T. Popa" Iasi, based on the contract no. 4872/18.03.2013 and the PN-II-ID-PCCE-2011-2-0028 Grant.

References

[1] N.C. Cook, S. Samman, J. Nutr. Biochem., **7**, 66 (1996).
[2] G. R. Beecher, J. Nutr., **133**, 3248 (2003).
[3] F. A. Fluckiger, D. Handbury, Pharmacographia - a history of the principle drugs of vegetable origin, International Book Distributors, Delhi (1986).
[4] A. Garg, S. Garg, L. J. Zaneveld, A. K. Singla, Phytother. Res., **15**, 655 (2001).
[5] G. Kaur, N. Tirkey, K. Chopra, Toxicology, **226**, 152 (2006).
[6] O. Benavente-Garcia, J. Castillo, J. Agric. Food. Chem., **56**, 6185 (2008).
[7] A. Balakrishnan, V. P. Menon, Fundam. Clin. Pharmacol., **21**, 535 (2007).
[8] M. Amiel, R. Barbe, Ann. Cardiol. Angiol., **47**, 185 (1998).
[9] C. Allegra, M. Bartolo, B. Carioti, D. Cassiani, Int. J. Microcirc. Clin. Exp., **15**, 50 (1995).
[10] H. K. Kim, T. S. Jeong, M. K. Lee, Y. B. Park, M. S. Choi, Clin. Chim. Acta., **327**, 129 (2003).
[11] M. Yamamoto, A. Suzuki, H. Jokura, N. Yamamoto, T. Hase, Nutrition, **24**, 470 (2008).
[12] H. Chiba, M. Uehara, J. Wu, X. Wang, R. Masuyama, K. Suzuki, K. Kanazawa, Y. Ishimi, J. Nutr., 133, 1892 (2003).
[13] V. Gaur, A. Kumar, Pharmacol. Rep., **62**, 635 (2010).
[14] T. Tanaka, Cancer Res., **57**, 246 (1997).
[15] A. Gil-Izquierdo, M.I. Gil, F. A. Tomas-Barberan, F. Ferreres, J. Agric. Food. Chem., **51**, 3024 (2003).
[16] D. K. Batt, K. C. Garala, J. Incl. Phenom. Macrocycl. Chem., **77**, 471 (2013).
[17] T. Loftsson, T. Jarvinen, Adv. Drug. Deliv. Rev., **36**, 59 (1999).
[18] E. M. M. Del Valle, Process Biochem., **39**, 1033 (2004).
[19] S. Gould, R. C. Scott, Food Chem. Toxicol., **43**, 1451 (2005).
[20] N. Qiu, X. Cheng, G. Wang, W. Wang, J. Wen, Y. Zhang, H. Song, L. Ma, Y. Wei, A. Peng, L. Chen, Carbohydr. Polym., **101**, 623 (2014).
[21] A. Corciova, C. Ciobanu, A. Poiata, C. Mircea, A Nicolescu, M. Drobota, C. D. Varganici, T. Pinteala, N. Marangoci, J Incl. Phenom. Macrocycl. Chem. **in press** (2014).
[22] T. Higuchi, K. A. Connors, Adv. Anal. Chem. Instr., **4**, 117 (1965).
[23] J. Hadžiabetdić, A. Elezović, O. Rahić, I. Mujezin, Am. J. Anal. Chem. **3**, 81 (2012).
[24] K. A. Connors, Thermodynamics of pharmaceutical systems: An introduction for students of pharmacy, John Wiley & Sons, Inc., Hoboken, New Jersey (2002).
[25] B. Liu, W. Li, T.A. Nguyen, J. Zhao, Food Chem., **134**, 926 (2012).
[26] C. Akbay, L. N. Gill, M. I. Warner, Electrophoresis, 28, 1752 (2007).
[27] T. Hatano, H. Kagawa, T. Yasuhara, T. Okuda, Chem. Pharm. Bull., **36**, 2090 (1988).
[28] M. Oyazu, Jpn. J. Nutr. **44**, 307 (1986).
[29] K. E. Malterud, K. M. Rydland, J. Agric. Food Chem., **48**, 5576 (2000).
[30] V. Kuntić, N. Pejić, S. Mićić, Acta Chim. Slov., **59**, 436 (2012).
[31] S. Tommasini, M. L. Calabrò, R. Stancanelli, P. Donato, C. Costa, S. Catania, V. Villari, P. Ficarra, R. Ficarra, J. Pharm. Biomed. Anal., **39**, 572 (2005).
[32] S. Majumdar, R. Srirangam, Pharm Res., **26**, 1217 (2009).
[33] C. O. Onyeji, S. I. Omoruyi, F. A. Oladimeji, Pharmazie, 62, 858 (2007).
[34] Z. Q. Yan, W. Wu, J. Sun, X. H. Liu, Y. P. Zhao, Y. H. Sun, T. Shang, Z. He, Drug. Dev. Ind. Pharm., 34, 632 (2008).
[35] V. B. Chaudhary, J. K. Patel, Int. J. Pharm. Sci. Res., 4, 68 (2013).
[36] S. Y. Lin, H. L. Lin, C. C. Lin, C. H. Hsu, T. K. Wu, Y. T. Huang, Thermodynamics – Physical Chemistry of Aqueous Systems, InTech, Rijeka (2011).

[37] A. Zoppi, A. Delrivo, V. Aiassa, M. R. Longhi, AAPS. Pharm. Sci. Tech., **14**, 727, (2013)
[38] H. Kim, H. W. Kim, S. Jung, Bull. Korean Chem. Soc., **29**, 590 (2008).
[39] Y. Zheng, A. H. L. Chow, Drug Dev. Ind. Pharm., **35**, 727 (2009).
[40] L. Wang, X. H. Jiang, W. J. Xu, C. R. Li, Int. J. Pharm., **341**, 58 (2007).
[41] J. Liu, L. Y. Qiu, J. Q. Gao, Y. Jin, Int. J. Pharm., **312**, 137 (2006)
[42] D. De Paula, D. C. R. Oliviera, A. C. Tedesco, M. V. L. B. Bentley, Braz. J. Pharm. Sci., **43**, 111, (2007).
[43] O. Aleem, B. Kuchekar, Y. Pore, S. Late, J. Pharm. Biomed. Anal., **47**, 535 (2008).
[44] G. C. Pupe, M. Villardi, C. R. Rodrigues, A. H. V. Rocha, L. C. Maia, V. Pereira de Sousa, L. Mendes Cabral, Int. J. Nanomed., **6**, 2581 (2011).
[45] W. L. Chaffin, Microbiol. Mol. Biol. Rev., **72**, 495 (2008).
[46] M. E. Carlotti, S. Sapino, E. Ugazio, G. Caron, J. Incl. Phenom. Macrocycl. Chem. **70**, 81 (2011).
[47] T. A. Nguyen, B. Liu, J. Zhao, D. S. Thomas, J. M. Hook, Food Chem., 136, 186 (2013).
[48] S. M. Gharibzahedi, S. H. Razavi, M. Mousavi, Carbohyd. Polym., **101**, 1147 (2014).
[49] I. Konczak, D. Zabaras, M. Dunstan, P. Aguas, Food Chem., **122**, 260 (2010).
[50] M. V. Kumaraswamy, S. Satish, Adv. Biol. Res., **2**, 56 (2008).
[51] L. Rackova, M. Oblozinsky, D. Kostalova, V. Kettmann, L. Bezakova, J. Inflamm**.** in press (2007).
[52] S. D. Bhise, Int. J. Res. Pharm. Biomed. Sci., 2, 596 (2011).
[53] T. E. G. K. Murthy, G. Sowjanya, Asian J. Biochem. Pharm. Res., **2**, 676 (2011).